

DARESBUURY LABORATORY
INFORMATION QUARTERLY
for
PROTEIN CRYSTALLOGRAPHY

An Informal Newsletter associated with Collaborative Computational Project No. 4
on Protein Crystallography

Number 15

July 1985

Contents

Laue photographs using Synchrotron

x-radiation

Report on a Daresbury Synchrotron Radiation

PX users meeting and additions

of work done since then

Editor: Pella Machin

Science & Engineering Research Council,
Daresbury Laboratory, Daresbury,
Warrington WA4 4AD, England

Deputy Editor
for Imperial
College: Dr. Alan Wonacott

Imperial College of Science & Technology,
The Blackett Laboratory, Prince Consort Road,
London SW7 2BZ

Deputy Editor
for Birkbeck
College: Dr. David Moss

Department of Crystallography, Birkbeck College,
University of London, Malet Street, London WC1E 7HX

Editorial

This edition of the newsletter contains a report of progress in the use of full white beam Laue photography on the Synchrotron Radiation Source (SRS) at Daresbury. The work was described at an SRS Protein Crystallography user meeting in April 1985 and will be published in more detail in the scientific literature at some future date. Anne Bloomer chairing the user meeting suggested that the topic is of general interest and should be circulated via this newsletter.

Pella Machin

THE LAUE METHOD - PROGRESS AND PROSPECTS

Laue photographs - stationary crystal, 'white' beam of radiation, in this case effectively $\lambda = 0.3$ to ca 2 \AA - were first taken on the protein crystallography Wiggler station on the SRS in June 1984, for the protein pea lectin and for several simpler crystals. Exposure times are very short (subsecond to 1 minute) and the number of reflections recorded per film very large; if intensities can be satisfactorily measured they offer exciting possibilities for studying changes taking place in crystals over short periods of time; they may also be useful for checking crystal quality and for some very small crystals.

At the protein crystallography user group meeting at Daresbury Laboratory in April 1985 the morning session was devoted to progress in these areas. The account given here is based on this session, but takes some material from a paper in preparation on the processing of intensity data from Laue photographs, and includes some other new material.

THE GEOMETRY OF THE LAUE METHOD

The geometry of the Laue method is illustrated in figure 1.

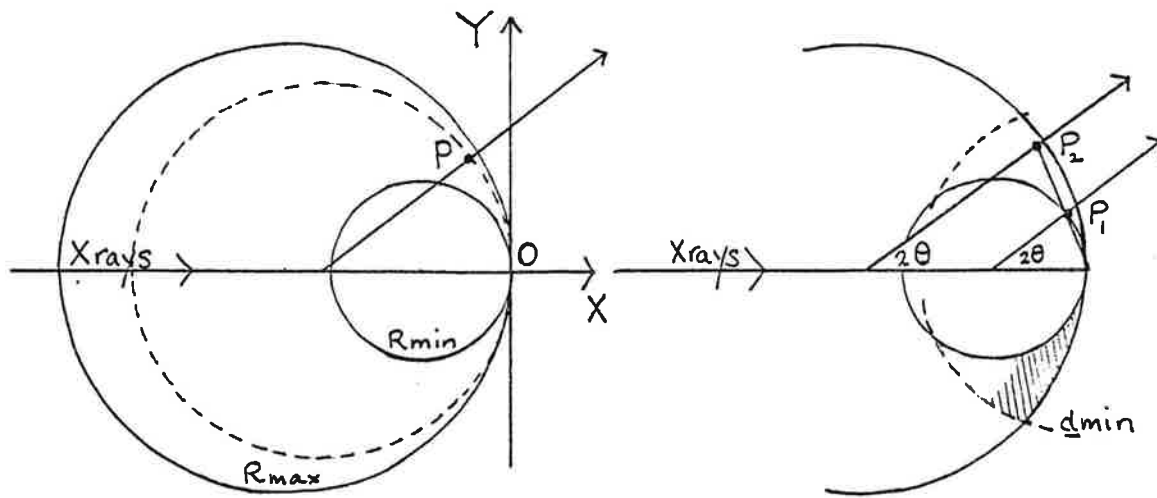


fig 1

fig 2

XYZ are orthogonal axes in reciprocal space, for a fixed wavelength, say 1.10 \AA ; conventionally Z is parallel to the spindle of the camera. The circles of radius R_{\max} and R_{\min} represent the spheres of reflection for the wavelengths λ_{\min} and λ_{\max} ($R_{\max} = 1.10/\lambda_{\min}$ here). Any reciprocal lattice point, eg P at x, y, z between these two spheres may then give rise to a reflection; the centre of the relevant reflection sphere is at $-R, 0, 0$ where

$$R = (x^2 + y^2 + z^2) / 2x$$

and the wavelength giving rise to the reflection is $1.10/R$. Fig 2 shows the reflecting spheres for wavelengths $\lambda_{\min} = 0.7 \text{ \AA}$ and $\lambda_{\max} = 1.8 \text{ \AA}$ and shows the region of reciprocal lattice covered if $d_{\min} = 2.0 \text{ \AA}$. It also shows one of the problems in using Laue patterns, that of 'wavelength overlaps'. The reciprocal lattice points P_2 and P_1 lie on a line which passes through the origin; these reflections will be superimposed in the Laue pattern since the angles of diffraction are the same for both. If the indices are h, k, l and nh, nk, nl then the wavelengths are related $\lambda_2 = \lambda_1/n$.

Some aspects of Laue patterns are illustrated in fig 3 and, for example high resolution (low d) reflections are not necessarily at the edge of the film.

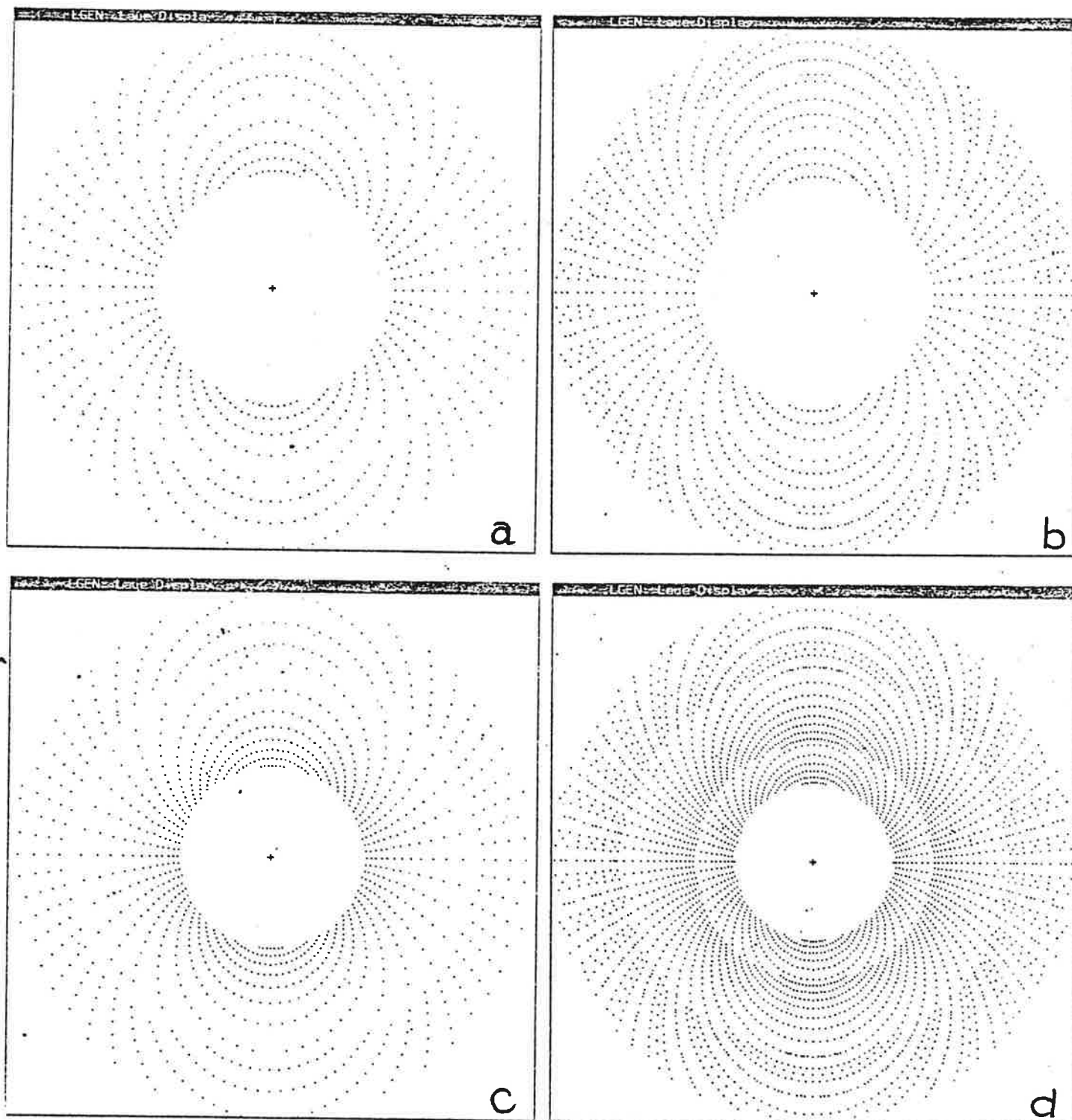


Fig 3 Predicted Laue patterns for a simple cell, showing the effect of varying the λ range and d_{\min} .

(a) λ 0.6 - 1.5, d_{\min} 1.4

(b) λ 0.6 - 1.5, d_{\min} 0.9

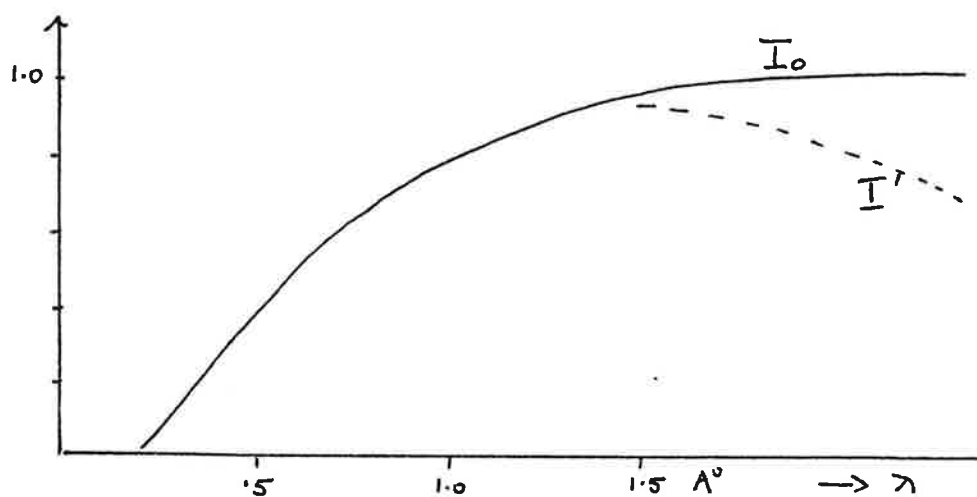
(c) λ 0.3 - 1.5, d_{\min} 1.4

(d) λ 0.3 - 1.5, d_{\min} 0.9

EXPERIMENTAL ASPECTS

On the SRS Wiggler beam line, station 9.6, it is possible to position the Arndt Wonacott Oscillation Camera to receive the full focussed white beam without monochromatisation; there are $\sim 10^{14}$ photons $\text{sec}^{-1} \text{mm}^{-2}$ in the wavelength range 0.5-2 Å. On beam line 9.7 (which has no focussing mirror) the carousel for 8 films cannot be accommodated but a single film cassette can be; $\sim 10^{13}$ photons $\text{sec}^{-1} \text{mm}^{-2}$ are available. The incident intensity as a function of wavelength is shown in fig 4. Laue patterns have been recorded in both these situations.

Fig 4 Relative intensity of SR Wiggler beam at different wavelengths (I_0) and after attenuation by Be windows and air path (I').

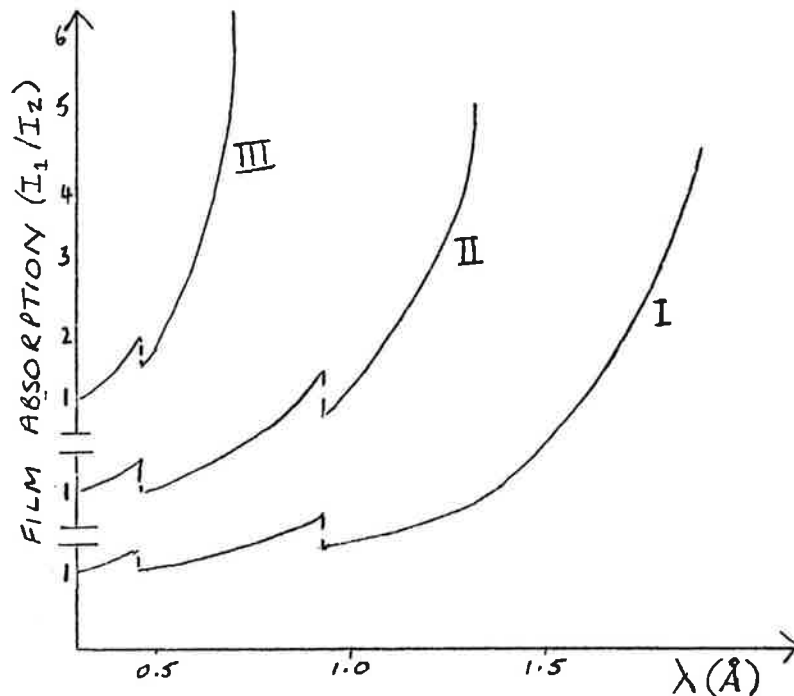


The different reflections in the Laue pattern result from different wavelengths present in the incident radiation. Intensity measurements must be made at different wavelengths. A composite film pack is used which makes wavelength discrimination possible for multiple reflections, as well as covering the dynamic range of the intensities at different wavelengths. A typical pack is:-

2 papers, F, F, Al, F, Al, F, Cu, F, Cu, F

where F stands for film (CEA reflex 25 used here), Al for aluminium foil of 150 μ thick, Cu for copper foil 38 μ thick. The properties of this pack are shown in fig 5.

Fig 5



Curve I is for two successive films with no separator
Curve II is for successive films separated by one Al foil
Curve III is for successive films separated by one Cu foil

The graph also illustrates two discontinuities that occur in the film absorption factor at the silver and bromine absorption edges.

The different wavelengths necessarily used affect the intensities through a variety of processes:-

- i The incident intensity in the SRS spectrum, as passed through focussing mirror, beamline windows, air path etc.
- ii Sample absorption (and capillary and liquid).
- iii Film factor, also obliquity, absorption by cassette paper.
- iv Source polarisation - the fractions $I_{||}$ and I_{\perp} depend on λ .
- v The Lorentz factor, $\lambda/\sin^2\theta$.
- vi Anomalous scatterers if present.

All these factors are dealt with at the normalisation stage of the processing described below.

OVERVIEW OF THE STAGES IN INTENSITY MEASUREMENT

After scanning all the films in each pack the stages in processing are:-

- a) Prediction of the Laue pattern to match the observed film.
- Refinement*
b) Integration of film density at predicted reflection positions, for all films in the pack.
- c) Derivation of interfilm scale factors, each of which is a function of wavelength, and scaling together of all films in the pack. The result must be $H K L F \sigma \lambda$ for each reflection (after l_p correction) [absorption should be dealt with here too]. This stage will involve a post refinement procedure to tweak up experimental parameters.
- d) 'Unscrambling' of reflection intensities which are harmonic overlaps - a method has been devised for doublets and triplets, but not yet tested.
- e) Normalisation to take account of the variation with wavelength of incident intensity and other factors listed above, and film response. For the test crystals we have been working with $F_{\text{Laue}} / F_{\text{mono}}$ may be plotted as a function of wavelength to derive the appropriate normalisation curve. When F_{mono} is unknown it will be necessary to record and process a Laue film pack from a standard crystal using the same SRS and camera conditions to establish the normalisation curve.
- f) Scaling and merging of film packs (as for monochromatic data)

Computer programs have been set up for each of these stages (except d) and applied to two test sets of films, from crystals for which monochromatic data is already available.

These crystals and data sets are:

'BPD' *

$C_{10}H_{15}N_2PS_3$, M.W. = 290

orthorhombic, $a = 15.037$ $b = 11.118$ $c = 7.818$ Å

space group $Pna2_1$, $Z = 4$

dmin 1.1 Å

6 film packs at 15° intervals around spindle

exposure time 5 sec for each

* trimethyl 1H-2,1,3 - benzophosphodiazine-4(3H)-thione 2,2 disulphide
from Colin Reynolds, York University and Liverpool Polytechnic.

Pea Lectin,

M.W. = 50000

orthorhombic, $a = 50.37$ $b = 60.58$ $c = 135.50$ Å

space group $P2_12_12_1$

dmin 2.6 Å

Film packs at 30° intervals around spindle, but crystal seriously
damaged by radiation by 12th pack. 5 packs were processed.

Exposure time 45 sec for each pack (SRS single bunch, unfocussed white
beam)

PREDICTION OF THE LAUE PATTERN

The positions of all reflections in a Laue diffraction pattern may be calculated given the dimensions of the unit cell and its orientation relative to the camera axes, the range of wavelengths present, λ_{\min} λ_{\max} , the crystal to film distance, and the minimum observable plane spacing, d_{\min} . In the prediction it is assumed that λ_{\min} , λ_{\max} and d_{\min} are sharp limits whereas in reality the incident or scattered radiation falls off continuously; they are initially adjusted to get the best match with the observed film pattern visually, after the orientation has been fixed. When a vertically focussing mirror is used λ_{\min} is a sharp parameter eg now it is 0.5Å.

An interactive computer program has been developed for the prediction and inspection of such Laue patterns. This software runs on an ICL PERQ computer and utilises the black and white raster screen (1024 x 760 pixels) for display, and the tablet and puck for fast interaction. The PERQ screen is subdivided for the simultaneous display of this input command menu, the resulting Laue pattern and numeric information about the reflections generated. Table 1 details how the number of reflections generated for a film of the Pea Lectin protein crystal varies with wavelength, showing the relatively large numbers of reflections in the lower wavelength ranges. It is also interesting to note the significant number of wavelength overlap spots which occur (for example 18 harmonics of 0 -1 1) as shown in Table 2 and hence the need to obtain the separate components of the intensity for the doublets at least and a technique for this analysis has been devised.

Program options are available which allow spot identification (x, y, h, k, l, λ) or the expansion of an area of the pattern for closer examination. Hard copy of the pattern may be obtained and it may be redisplayed to show a selection of spots, for example the wavelength overlap spots where different harmonics are superimposed, or alternatively spots which are spatially well separated. Some example plots are shown at the end of this paper.

The software has proved most useful as an educational tool and for the examination of the effects of changing of parameter values, as well as for the basic prediction of the Laue pattern which is required as an initial step in the intensity measurement process.

Table 1

<u>Pea Lectin ($\phi = 30^\circ$ Pack 9)</u>		<u>BPD ($\phi = 180^\circ$ Pack 22)</u>	
<u>(\AA)</u>	<u>Number of reflections</u>	<u>(\AA)</u>	<u>Number of reflections</u>
0.48	1017	0.46	101
0.63	1059	0.62	116
0.78	1036	0.78	114
0.93	1043	0.94	107
1.09	1056	1.10	116
1.24	1030	1.26	75
1.39	1038	1.42	30
1.54	936	1.58	31
1.69	626	1.74	17
1.84	454	1.90	14
1.99	315	2.06	14
2.15	249	2.22	4
2.30	175	2.38	6
2.45	134	2.54	6
2.60	102	2.70	0
TOTAL	10270	TOTAL	751

Table 1 shows for both test data sets the variation of the numbers of reflections generated with wavelength.

Table 2

<u>Pea Lectin Data</u>		<u>BPD</u>
<u>Number of reflections</u>	<u>Multiplicity</u>	<u>Number of reflections</u>
	<u>of reflection</u>	
7922	1	554
729	2	62
156	3	14
43	4	1
22	5	4
2	6	-
5	7	1
5	8	
-	9	
1	10	
-	11	
1	12	
1	13	
-	14	
-	15	
-	16	
-	17	
1	18	
	19	
	20	

Table 2 Distribution of multiply recorded (harmonic) reflections

Note The singlets originate principally from the low d spacing (high resolution reflections. The large d spacing reflections ($5\text{\AA} - 00$) are usually multiplet. The 'unscrambling' of harmonics to give the lower resolution data is likely to be important.

PARAMETER REFINEMENT

Before accurate intensity measurement can be attempted, it is essential to adjust the predicted spot positions till they exactly match the experimentally observed positions.

The crystal orientation may not be known very accurately and it is necessary to refine 3 angles to allow for such crystal missetting. It is also necessary to refine parameters which allow for geometric distortions and we have found a 10 parameter (3 missetting angles, x y film centre, crystal to film distance, twist, tilt, bulge, y scale) least squares refinement procedure to be satisfactory.

The observed spot positions may be obtained by displaying the experimental data (in this case a digitised photographic film) on, for example, a tektronix type computer graphics terminal, as a background corrected threshold plot, and identifying a particular spot with the cursor, and using a centre of gravity calculation on the data in that region to obtain an accurate position of the nearest intensity peak. This process may be repeated for several spots. In practice it is best to use spots which are spatially isolated and it is interesting to note that the reflections which are most useful at this stage for refining the geometry are the wavelength overlap spots containing several harmonics.

INTENSITY MEASUREMENT

The problems of obtaining background corrected intensity measurements from Laue data are very similar to those experienced when using other camera geometries. Three particular features are worth mentioning: the spot shape varies rapidly; the spots (for protein films) may be extremely close especially along lunes of data, thus causing difficulties during intensity measurement; though the wavelength overlap spots do not pose integration problems they do require subsequent deconvolution into separate components.

We have modified the MOSFLM program (ref. Evaluation of Integrated Intensities on Oscillation Photography - A. J. Wonacott) for the evaluation of intensities from white beam Laue photographs. The main modifications were:

- 1) Extension of the input "generate file" of reflection indices and spot coordinates to include additional parameters in the header records and to allow space to store the wavelength of each reflection and intensity measurements for up to 6 films.
- 2) Initial parameter refinement was based on nodal spots (isolated wavelength overlap reflections).
- 3) A square box was used for spot integration because of the significant variation in spot shape over the film.

A profile fitting option was introduced to improve intensity measurement in particular for spatially close spots. A gaussian spot shape of the form

$$I = P_1 \text{Exp} \left(- P_2(x-P_8)^2 - P_3(y-P_9)^2 - P_4(x-P_8)(y-P_9) \right)$$

was used to represent a peak centred on coordinates P_8, P_9 with peak height P_1 . A background plane of the following form was assumed

$$I_b = P_5 + P_6x + P_7y$$

The 9 parameters were refined for each spot using a modified Gauss-Newton algorithm for finding the unconstrained minimum of a sum of square of nonlinear functions.

The profile fitting option was used for about 70% of the data on a given film, the remaining spots being too weak to be fitted properly. The results on the Pea Lectin data showed that the internal symmetry agreement R factors on a film were improved by about 2% (6% reduced to 4% when profile fitting was used). This procedure needs to be extended so that learnt profiles from the strong reflections could be used to fit the weak data.

SCALING WITHIN FILM PACKS

Inter-film scale factors of the form

$$I_1 = I_2 e^{a\lambda^3}$$

have been assumed. Three wavelength ranges are needed ($\lambda < 0.49$, $0.49 < \lambda < 0.92$, $\lambda < 0.92$) because of discontinuities in the curve at the Ag and Br k edges, 0.49 Å and 0.92 Å; the coefficient 'a' is evaluated for each range. The starting values of the coefficients are set to the calculated values for the absorption of film emulsion, film + aluminium foil, and film plus copper foil, and then refined by an iterative process. Some reflections are actually harmonics although not predicted as such at this stage, because their wavelength or d-spacing lies just outside the 'hard' limits assumed; these reflections are detected since I_1/I_2 does not conform to the curve for the majority of reflections, and are rejected from the evaluation of coefficients. This affects particularly the scale factor at high λ values.

WAVELENGTH NORMALISATION

The calculation and application of the normalisation curve are done as follows. The data are divided into a number of wavelength bins and the ratio of the mean Laue intensity to the mean reference intensity is calculated for each bin. The points formed by this ratio as a function of wavelength are fitted by calculated curves using Chebyshev polynomial curve fitting routines from the NAG library (Nottingham Algorithms Library). To allow for discontinuities in the function of scale factor against wavelength (eg at the Silver and Bromine absorption edges), the scaling may be divided into a number of wavelength ranges. The program produces various analyses of the data.

MULTIPLE PACK SCALING AND MERGING

Several packs of normalised Laue data may be scaled to each other using a program such as ROTAVATA; it calculates scale and temperature factors between overlapping batches of reflection data by the method of Fox and Holmes (ref. Acta Cryst. (1966), 20, 886). The scale factor for the i 'th batch is given by the expression

$$K(i) = C(i) * \exp(-2*B(i)*\sin(\theta/\lambda)**2)$$

The scale and temperature factors $C(i)$ and $B(i)$ are relative to some specified batch for which the values are set to 1.0 and 0.0.

The batches of data are then merged as for conventionally measured reflection data using a program such as AGROVATA (ref. CCP4 program suite, Daresbury Laboratory).

SAMPLE RESULTS

The results obtained so far with the two test data sets illustrate the quality of the data and some of the problems.

Table 3 summarises the kind of data which is required at the prediction stage, the particular values used for the two test data sets, and the resulting number and type of reflections generated.

Profile fitting was applied to a test pack of the Pea Lectin data and one of the six film packs of the BPD data. As mentioned before it appears that profile fitting has the effect of improving the R_{sym} s from 6% to 4% so is clearly worthwhile (but was not always carried out for expediency at this test stage). In addition, when extended to the weak data it would help to reduce the R_{sym} further.

Table 3. Summary of typical data used to predict the Laue X-ray diffraction pattern with details of the number and type of spots generated for each of the two test data sets.

<u>Pea Lectin (Pack 9) ($\phi = 30^\circ$)</u>	<u>BPD (Pack 22) ($\phi = 180^\circ$)</u>
a = 50.37 Å	a = 15.037 Å
b = 60.58	b = 11.118
c = 135.50	c = 7.818
crystal to film 95.1 mm	38.59 mm
d min = 2.6 Å	1.1 Å
λ min = 0.33 Å	0.3 Å
λ max = 2.6 Å	2.7 Å
spot = 0.55 mm	0.9 mm
overlap criterion	
Total Number of spots generated 9389	724
Spots with no overlap 4170*	475
Spots with λ overlap 2177	184
Spots with both type of overlap 612	0
nodal spots 54	65

* used a larger box than was really necessary

Table 4

Summary of R factors for the 2 test data sets

	<u>Pea Lectin</u>	<u>BPD</u>
1. R_{sym} (on I) within the top film (for identical λ pairs)	4%	4 - 9%
2. Film to film scaling R_{scale} (on I) within one pack	8%	8 - 10%
3. Normalisation R (on I) I_{Laue} to I_{mono} within one pack	-	12% (10 - 16%)
4. Merging of packs R_{merge} (on I)	12%	13%
5. Agreement with monochromatic data R_{mono} (on F)	11%	11%

where

$$R_{\text{sym}} = \frac{\sum_{hkl} \sum_n (I_{hkl} - \bar{I}_{hkl})}{\sum_{hkl} n \bar{I}_{hkl}}$$

and

$$R_{\text{mono}} = \frac{\sum (F_{\text{mono}} - F_{\text{Laue}})}{\sum F_{\text{mono}}}$$

A summary of the processing statistics for the two data sets is given in Table 4. These give an indication of the quality of the data, but at this stage are preliminary. The range of values for BPD shows the variation from pack to pack and without exception the minimum R factor is for the pack processed with profile fitting. The final agreement of 11% between F_{Laue} and F_{mono} for Pea Lectin may usefully be compared with 8% obtained in a comparison between the monochromatic data set collected with Synchrotron Radiation to that collected with a conventional Cu K α source. At the moment it would appear that reasonable statistics may be obtained for measurements within a film or even film pack, but that there is room for improvement in the agreement of Laue data (after scaling and correction factors) with the standard monochromatic data. We do believe it is important that λ normalisation scale factors are derived statistically using large numbers of reflections per bin. At this stage comparisons of differences between similar Laue packs (for example in time resolved experiments) could be more profitable than the comparison of the finally corrected normalised data sets. Improvements are still being made in the later stages of data analysis. Certainly we are confident that white beam Laue photography on the Synchrotron offers an exciting new area of investigation and promises to be a useful scientific technique.

KINETIC LAUE PHOTOGRAPHY IN THE STUDY OF ACTIVITY IN TETRAGONAL
PHOSPHORYLASE B CRYSTALS (WORK OF J HAJDU AND D STUART)

We have recently been able to collect, conventionally, data sets at the SRS in 20-30 minutes enabling us to study the catalytic reaction of phosphorylase in the crystal. These studies have been very rewarding but do not provide sufficient time resolution to be entirely satisfactory.

In an effort to radically increase the rate of data collection we have explored the possibility of using the extreme power of the white (polychromatic) beam from the Wiggler magnet at the SRS to take Laue photographs of the tetragonal phosphorylase crystal. Initial experiments were very encouraging indicating the exposure times of less than one second would be required and also that we might hope to obtain several photographs from one position of the crystal. We have therefore designed and performed Laue experiments to study the reaction in the crystal.

There were some interesting aspects to the experimental design.

- i) Consideration of the symmetry of reciprocal lattice and the volumes of reciprocal space accessible with the Laue method led to the observation that it is possible to define optimal crystal settings. Figure 6 illustrates this for our experiments. We decided in the first instance to perform the experiment at one crystal orientation only although this restricts the data observable to less than the complete unique portion.
- ii) The experimental sequence. An example is shown in Figure 7. The rationale for the soaks was the same as for the rapid rotation camera data collection scheme. The experiment was performed using a flow cell and at 3°C. The orientation of the crystal was identical for all the exposures of one series, except for frequent translations along an axis normal to the beam. Because of the small size of the beam (200 μm diameter) many such translations could be performed on each crystal. In Fig 7 the switch from up arrows to down arrows occurs where the crystal was translated. A typical exposure time was 250 μmsec . (with the SRS operating at 2 GeV, over 100mA and the Wiggler at 5 Tesla). These small exposures were controlled by a specially designed shutter driven by the flash synchronization output of a standard 35mm camera.

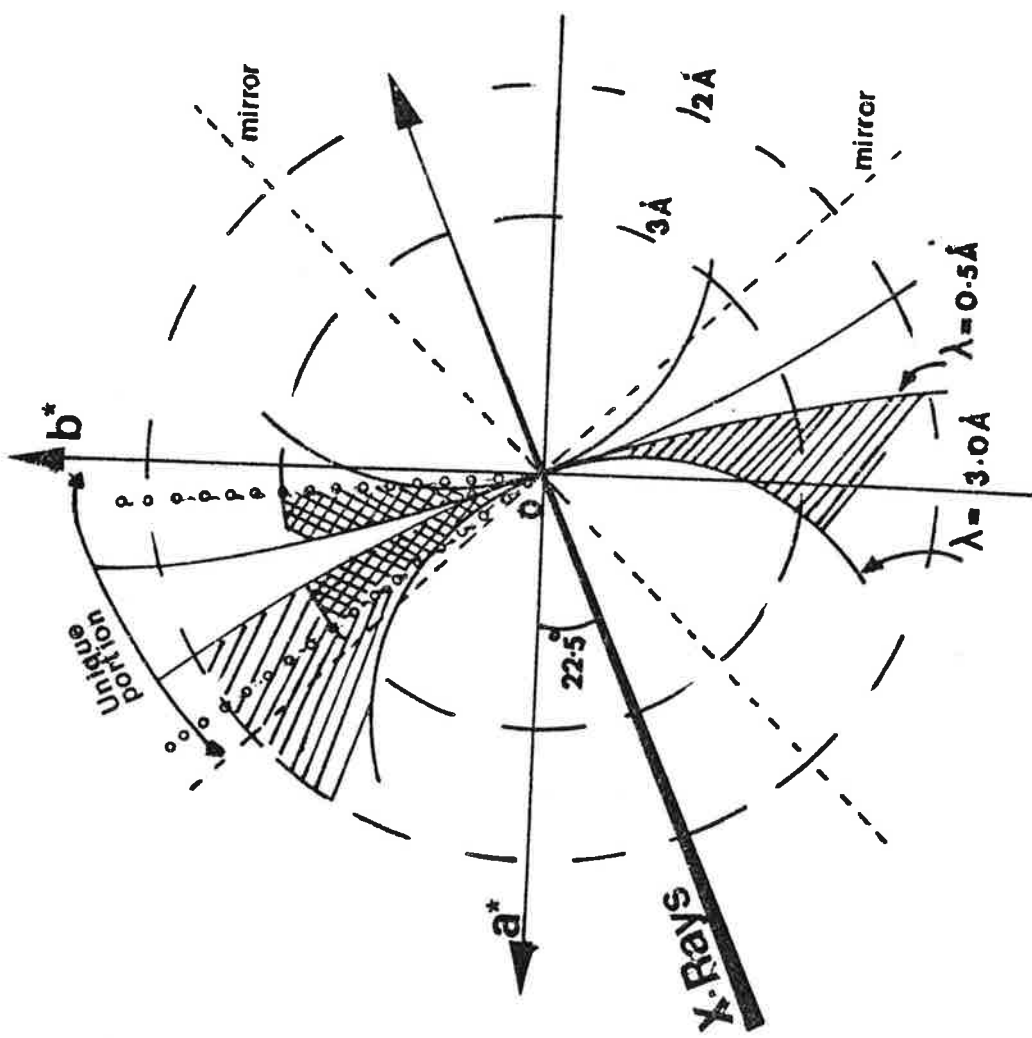


Fig. 6

KINETIC LAUE EXPERIMENT ON PP_b

50 mM G7, 2mM IMP
10mM BES-Mg, pH6.9

500 mM P_i
50 mM G7
2 mM IMP
pH 6.9

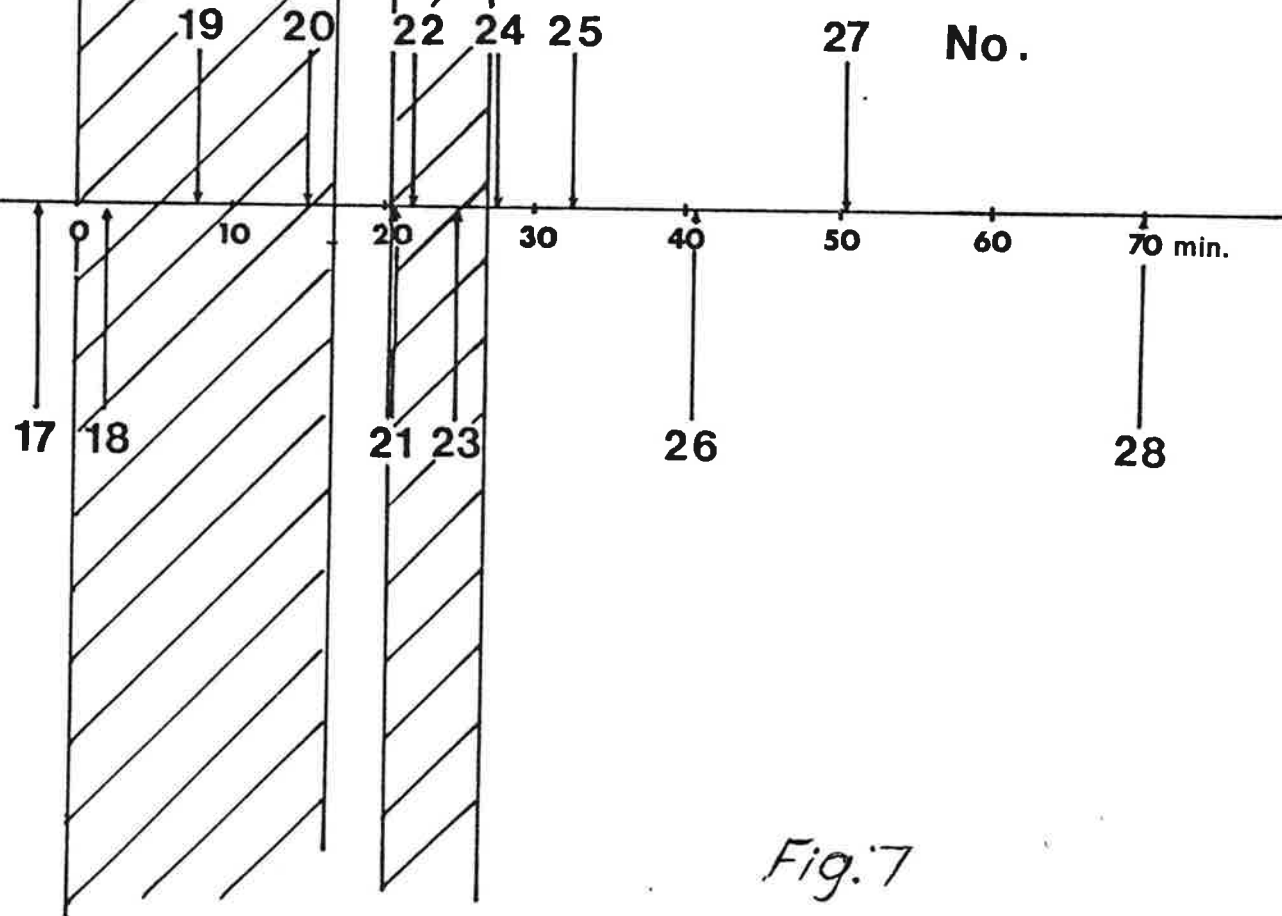


Fig.7

Each film pack consisted of 6 films interleaved with 3 Al foils and one Cu foil to increase the dynamic range and perhaps allow subsequent deconvolution of superimposed harmonics.

It is hoped that since the beginning of the sequence represents the native protein the individual Laue intensities may be normalized to these (separately for each film in the pack) and the same (or closely similar) normalization factor applied to each photograph in the experimental series.

A number of Laue sequences have now been recorded, both with the protocol described above and also for caged phosphate. At present the analysis of the photographs is still at an early stage although many of the computer programs necessary are now almost complete. It is not yet clear whether the data will be obtainable in sufficient quantity or quality to produce interpretable difference maps. It seems that up to about 34,000 reflections are recorded on each photograph, of which some 25% occur as harmonic overlaps and some 15% as spatial overlaps. This leaves some 60% of the data as potentially measureable as non-overlapping. It will be interesting to see how many reflections can in fact be reliably estimated.

APPLICATION TO VERY SMALL CRYSTALS

Some progress has already been made in using the high intensity of SR in monochromatic oscillation photographs to record data on very small crystals, with all dimensions less than ca 50 μ ; the compounds studied so far have been of small molecular weight. The possibility of using Laue diffraction patterns for recording data on such crystals seemed ideal, since exposure times should be short (≤ 1 min) and a full sphere of data could be recorded in 6 - 10 exposures. To our disappointment when Laue photographs were taken for a number of different samples (see Table 5) in most cases the reflections were substantially streaked or spread compared with those in protein photographs or from other crystals of 'conventional size'. This is attributed to mosaic spread within these crystals, or some disorder in the orientation of small crystallites. Unfortunately the effect on spot shape in the Laue photographs is such that accurate intensity measurements by densitometry are not likely to be practicable in many cases.

THE EFFECT OF MOSAIC SPREAD IN LAUE PHOTOGRAPHS

Mosaic spread converts each reciprocal lattice point P into a small spherical cap (of a sphere with radius d^* and centred at the reciprocal lattice origin). The component, η_A of the mosaic spread, which is in the plane X, Y, in Fig 8, results in a radial extension of the Laue diffraction spot on the film, $2\eta_A * D / \cos^2 2\theta$; the wavelength changes along the streak. The component, η_B , which is normal to this plane, results in a broadening of the streak, $2\eta_B * D * \sin\theta / \cos 2\theta$. Fig 9 shows these two effects. (The Laue diffraction geometry has cylindrical symmetry about the X-ray beam direction).

Observations on a variety of crystals are summarised in Table 5:

- a) In normal sized crystals of simple compounds and in normal sized fresh protein crystals the Laue spots are small, roughly circular, and of a size determined by the collimator (usually 0.2 or 0.3 mm here), and the beam divergence. Mosaic spread, η , estimated during the processing of monochromatic oscillation photographs is typically $\sim 0.1^\circ$, quite consistent with the spot size.

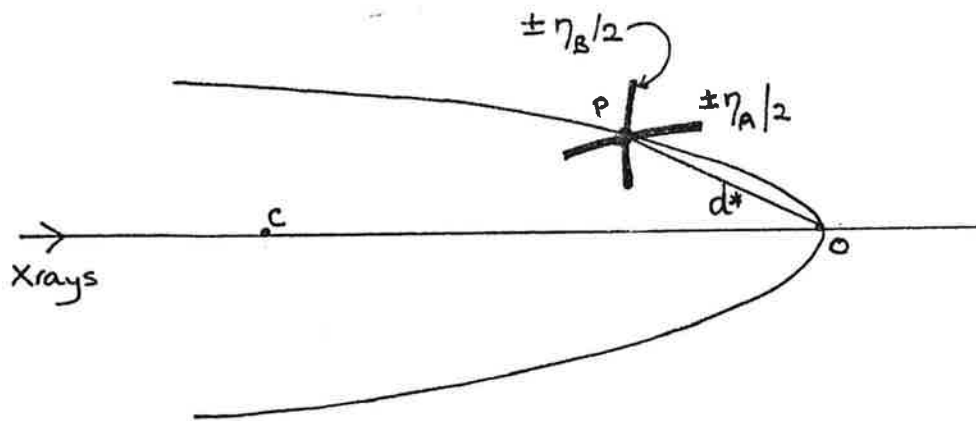


Fig 8 Components of Mosaic spread for reciprocal lattice point P. η_A is in the plane of P, the reciprocal lattice origin (O), and the centre of the reflecting sphere (C); η_B is normal to this plane. The displacement η_A requires a significant change in wavelength for reflection, and in radius of the reflecting sphere.

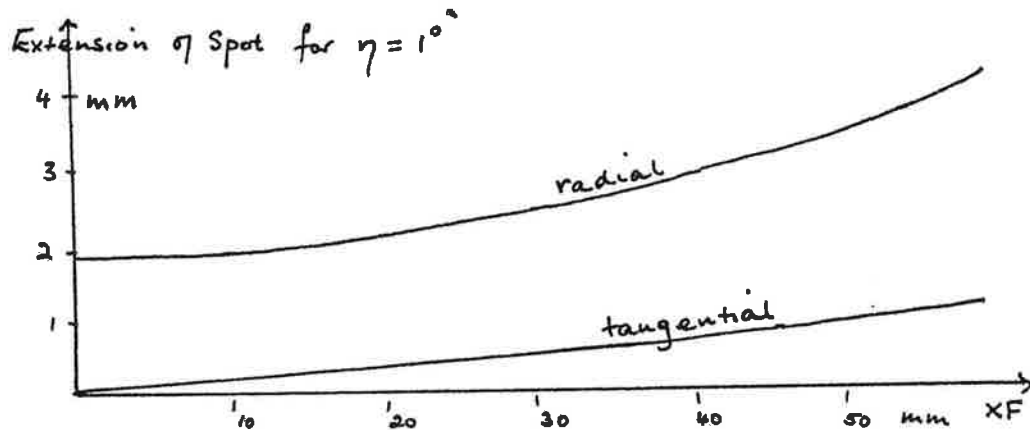


Fig 9 Extension of Laue reflection for a total mosaic spread $\eta = 1^\circ$ (which will usually be considered as $\pm\eta/2^\circ$). Crystal film distance = $D = 55\text{mm}$.

Table 5 - Summary of observations on Laue spot size and shape

Sample	Crystal size μm	Laue spot, size* and shape	Mosaic spread from graph
'normal' sized eg ammonium oxalate eg fresh protein	300 x200 x100	~ circular, .15-.2 mm (diffuse haloes around very intense spots)	[0.1°]
radiation damaged protein crystal eg tetragonal Lysozyme	same	streaked or extended spots in some cases ellipses up to 0.5-1mm	0.2-0.4°
very small crystals eg disaccharide 1) 2) ammonium oxalate	150x25x5 250x20x20 40x40x20	streaks or ellipses ~ 1.5 x 0.1 mm ~ 3.5 x 0.3 mm ~ 1 x 0.1 mm	~ 0.6° ~ 1.5° ~ 0.4°
proflavine hemisulphate chip of larger 'good' crystal	~ 40x40x40	small sharp round spots < ~ .2 mm	[0.1°]

* for crystal film distance 55 mm, $\theta \sim 25^\circ$, a visual estimate, and a little dependent on spot intensity

b) Protein crystals which have suffered radiation damage, show in most cases substantially elongated or streaked spots. It appears that one of the effects of the radiation is to increase mosaic spread, to values such as 0.4° .

c) Some very small crystals show sharp radial streaks, for others the spots appear to be composite, made up of a number of smaller streaks, spread over a larger area of film and corresponding in total extent to 1° - 2° in angles between constituent crystallites. All these cases are either small crystals in batches where some others have grown larger, or small crystals of compounds which had never yielded larger crystals. It is likely that the poor ordering of crystallites, as indicated by large mosaic spread, has prevented these nuclei from growing to larger crystals.

d) Two very small crystals of proflavine hemisulphate, chipped from a much larger crystal, gave very small sharp Laue reflections, corresponding to small mosaic spread like the crystals in (a).

Summary

Laue diffraction photographs of proteins and other simple compounds have been taken on the SRS. Suitable multiple film packs allow discrimination of wavelengths and measurement of intensities of the reflections. Programs have been developed, or existing programs modified for 1) prediction of Laue patterns for a given cell and orientation, and refinement to match observed pattern, 2) intensity measurement from densitometered film record, 3) scaling together of films within a pack, where scale factors are wavelength dependent, and 4) normalisation of the intensities to correspond to measurements made at a single wavelength. The application to Laue photographs from two test crystals, a protein and a smaller organic molecule, is described and indicates the quality of the data.

Other applications of Laue photography include a) a kinetic study of a reaction catalysed by phosphorylase, and b) assessment of crystal quality; most very small crystals studied show substantial streaks in their Laue diffraction patterns rather than sharp spots; these may be related to mosaic spread to which the Laue geometry is particularly sensitive.

This report has been assembled by Pella Machin and Marjorie Harding but the work and contributions are from many people:

John Helliwell	Mike Elder	Marjorie Harding
Miroslav Papiz	Pella Machin	Janet Hails
Steve Rule	John Campbell	Steve Andrews
George Habash	Ian Clifton	
Durward Cruickshank		

LAUE PATTERN PREDICTION on the PERQ computer for the protein PEA LECTIN

a=50.7 b=61.2 c=136.7

Wavelength cutoffs min=0.3 max=2.4 A

Sample resolution limit of 2.6 A assumed

a) The complete pattern generated. Total number of spots is 10494.

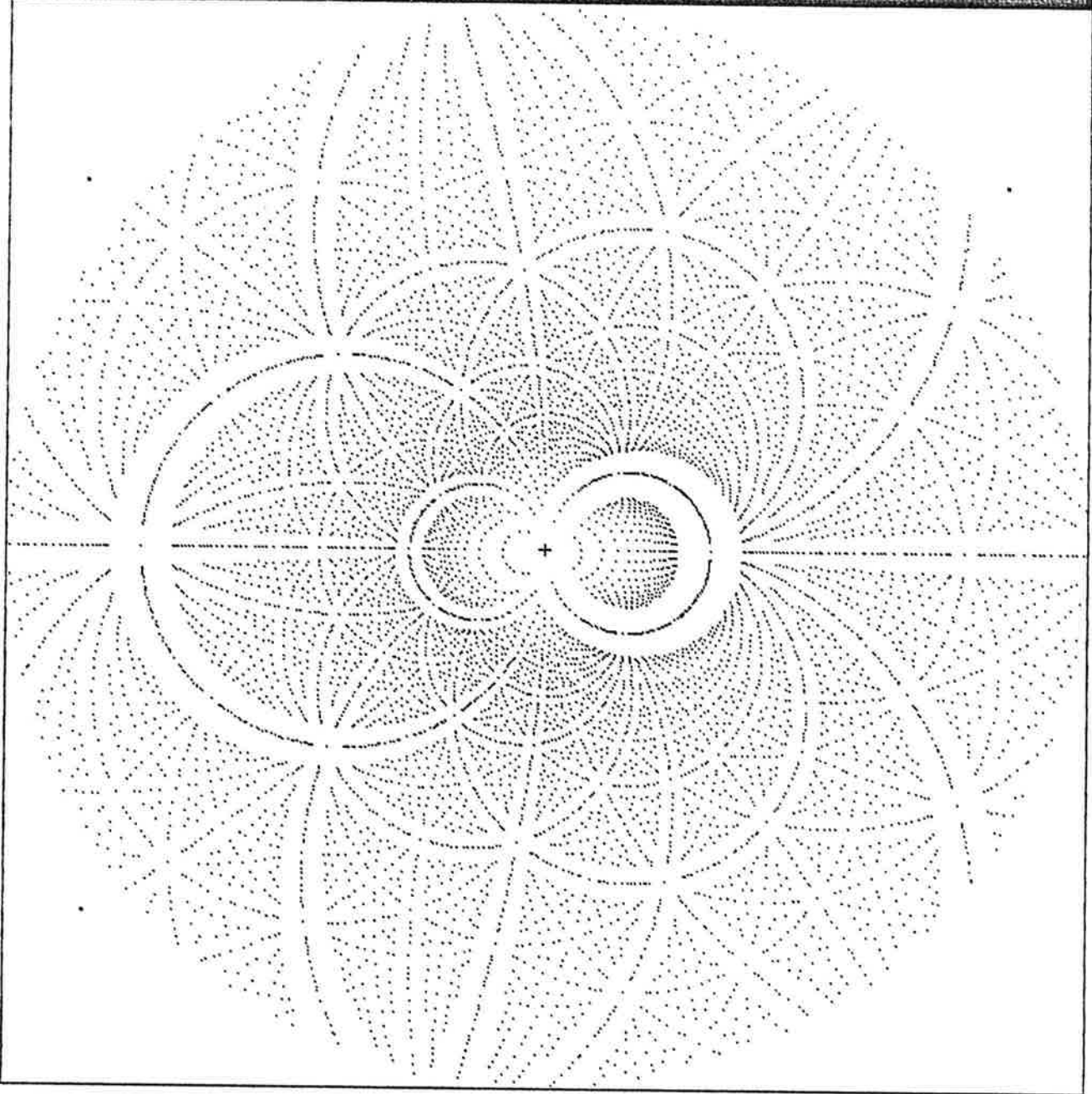
b) Measurable spots (omitting overlaps) (7112 spots)

c) Wavelength overlap spots (2247)

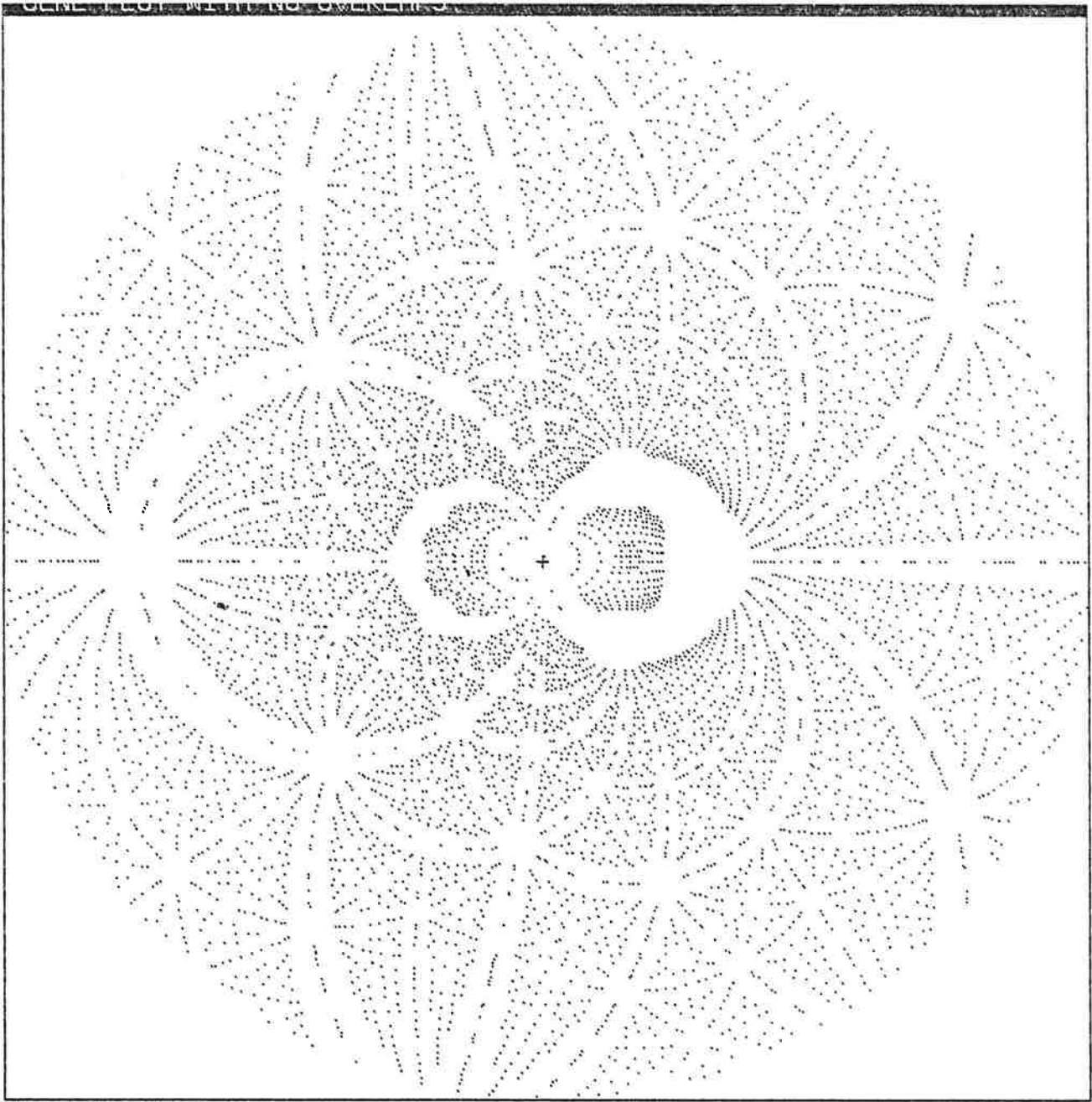
d) Spatial overlap spots (1320)

e) Spots with both wavelength and spatial overlaps (185)

LEGEND: Laue Display

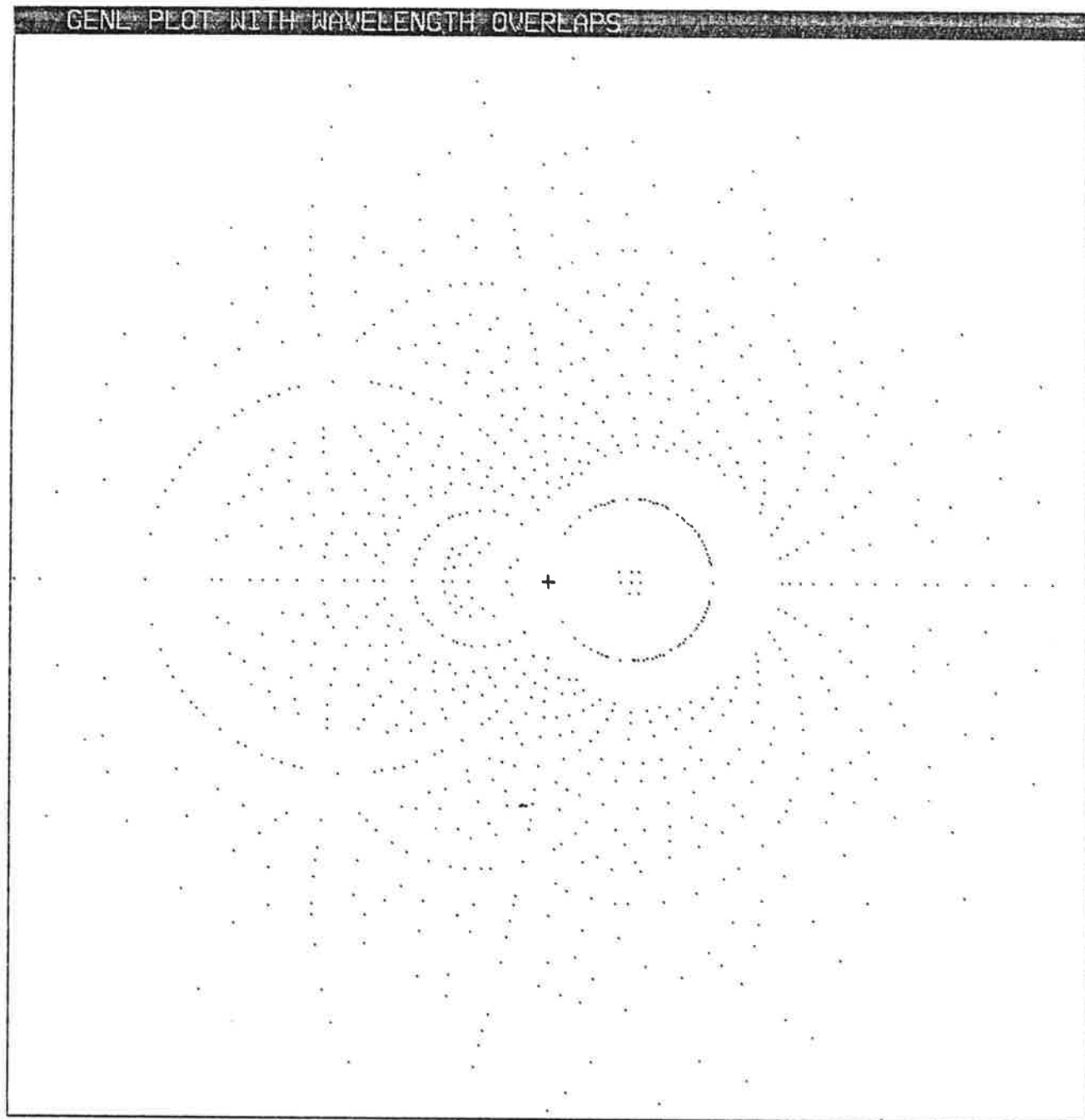


(a)



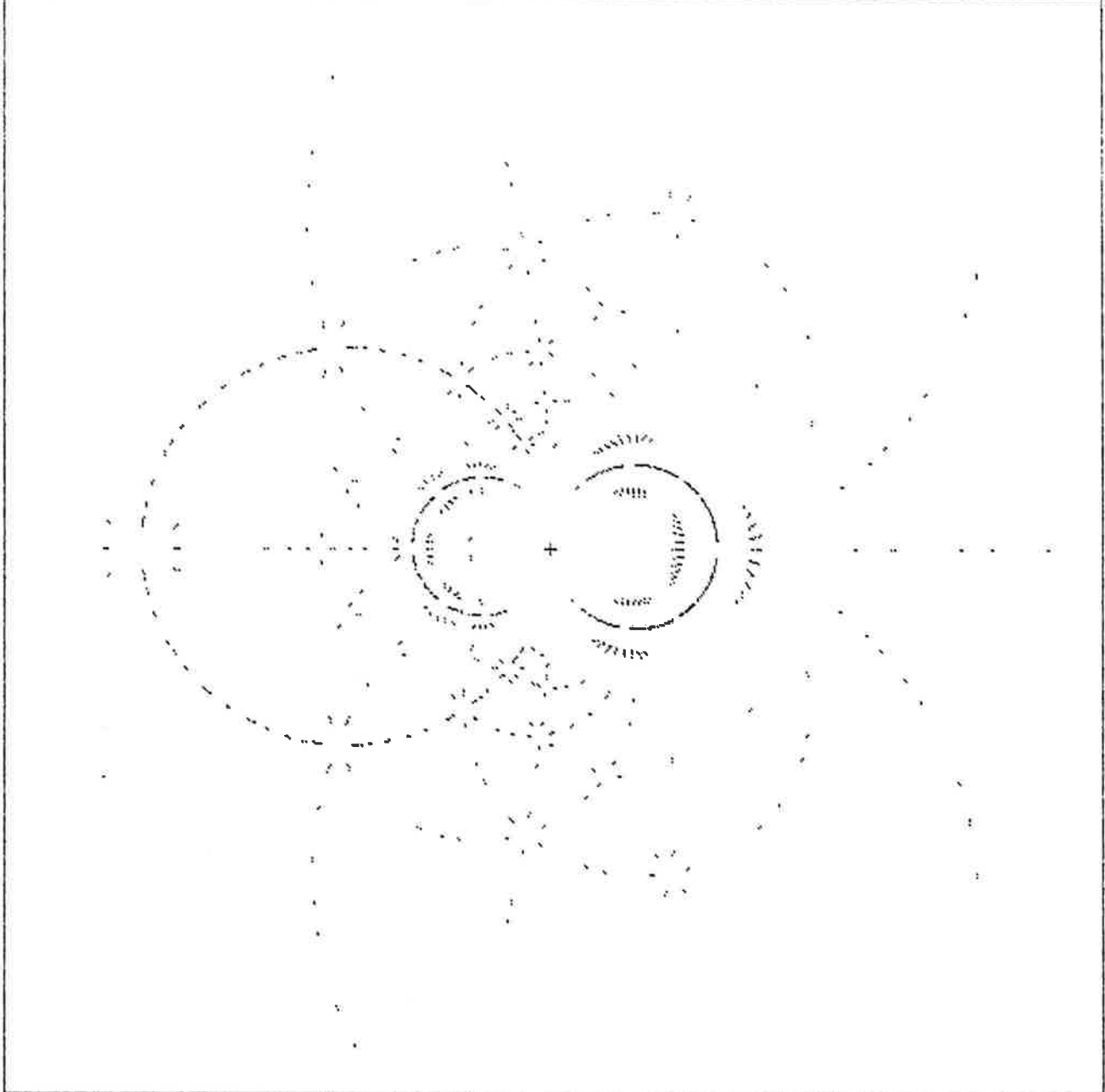
(b)

GENL PLOT WITH WAVELENGTH OVERLAPS



(c)

GENL PLOT WITH SPATIAL OVERLAPS



(d)



(e)

